Nonisotropic Mass Transfer Model for Green Bean Drying

C. Rosselló,*,† S. Simal,† N. SanJuan,‡ and A. Mulet‡

Department of Chemistry, University of Illes Balears, Ctra. Valldemossa km. 7.5, 07071 Palma de Mallorca, Spain, and Food Technology Department, University Politècnica, Cno. Vera s/n, 46071 València, Spain

Two diffusional models were developed for finite cylindrical shaped bodies which take into account that mass transfer could have a nonisotropic nature. In the first model, sample shrinkage was ignored; thus, it was solved by the separation of variables method. This hypothesis of constant sample volume was not assumed in the second model, which solved mass transfer equations through a finite difference scheme. The proposed models were applied to the simulation of drying curves of green beans (*Phaseolus vulgaris*). Two different effective diffusivity coefficients, one radial and the other axial, as a consequence of the mass transfer through both directions, were estimated in each model. The effective diffusivities estimated with the proposed models varied with the temperature according to the Arrhenius law. The average percentage of variance explained by the fixed boundaries model was 96.1% and increased to 99.1% when shrinkage was considered (in the model solved by a finite difference method).

Keywords: *Drying models; nonisotropic mass transfer; green bean; shrinkage*

INTRODUCTION

Mass transfer phenomena are extremely important in food processing, especially in drying and related operations. Suitable knowledge and control of mass transfer are essential to both the quality of the product and the economics of the process. The difficulties of applying transport phenomena theory to food processes arise from the complex physical structure and chemical composition of foods, which may vary even within the same food sample and may change during processing.

In that context, mathematical models representative of mass and heat transfer seem to be necessary for the analysis and design of a drying process. The complexity of the appropriate model depends on the purpose of the application considered (Kiranoudis et al., 1992).

The water transport phenomenon is rather complicated, as the moisture transfer may occur by different mechanisms. When external resistance to mass transfer is negligible at experimental conditions of air temperature and air flow rate, the usual treatment of the experimental results involves the assumption that the drying process is controlled by internal diffusion (Ketelaars et al., 1995). Usually, an apparent diffusion coefficient is measured. Under these circumstances, many models have been developed for biological materials using Fickian diffusion as the basis for the mass transfer mechanism (Jayaraman and Das Gupta, 1992). For processing purposes, the material is commonly cut into spheres, cylinders, cubes, or slabs. When the shrinkage that takes place during drying time is considered negligible and the diffusion coefficient is constant, models have an analytical solution (Rosselló et al., 1992). The main advantage of this kind of model is its simplicity.

In the case of high moisture content materials, the presence of a significant shrinkage has been reported. In fact, moisture gradients within the particle induce microstructural stresses leading to shrinkage (Aguilera and Stanley, 1990). This shrinkage of the sample during drying is usually assumed to be linearly proportional to the change in moisture content (Vagenas et al., 1990). Finite element (Vanegas and Marinos-Kouris, 1991; Jomaa et al., 1991) and finite difference (Fusco et al., 1991; Schrader and Litchfield, 1992) methods have been reported in the literature to solve the differential equations describing the moisture transfer in a moving boundary problem.

The drying phenomenon is often modeled by assuming that the process is of an isothermal type. This assumption implies that during dehydration of food products, heat transfer occurs very quickly (Yoshida et al., 1990).

Usually in drying modeling it is assumed, for the mathematical analysis, that the apparent moisture diffusion coefficient is the same in all directions (isotropic material) (Vanegas and Marinos-Kouris, 1991). Nevertheless, Koponen (1987) proposed a method for determining moisture diffusion coefficients of wood and found significant differences between the figures obtained for the radial and axial migration. Mounji et al. (1991) modeled the wood drying process in three dimensions using a finite differences method, based on the assumption that the sample was an anisotropic material with three principal axes of diffusion.

These findings pointed out that knowledge of microstructural arrangement of an heterogeneous food would be expected to lead to the improvement of physical models and to a better simulation (Aguilera and Stanley, 1990). Green bean (*Phaseolus vulgaris* L.) is a cylindrical shaped food with high moisture content (ca. 90%) and a significant fiber content (of complex composition, mainly lignin and cellulose) (ca 3.0% wm) (Holland et al., 1991), producing an oriented food structure due to the arrangement of the tissues.

The basic aim of this paper was to present a mathematical description of drying kinetics in the falling rate period for cylindrical shaped materials considering sample shrinkage and nonisotropic transport. For this purpose, two different diffusive models were developed and applied to drying of green beans. It seems useful

* Author to whom correspondence should be addressed.

† University of Illes Balears.

‡ University Politècnica.

S0021-8561(96)00534-1 CCC: $14.00

to consider models with different degrees of complexity to evaluate if the additional precision obtained compensates for the required effort and manages the complexity more efficiently. The complexity of the models and the need to consider the above-mentioned phenomena were evaluated.

MATHEMATICAL MODELS

Water transport could be described by considering Fick's law in an unsteady state mass balance which, in the case of a finite cylinder, can be written (Welty et al., 1993):

$$\frac{\partial W_l}{\partial t} = \left[D_{\mathrm{r\ eff}}\left(\frac{\partial^2 W_l}{\partial r^2} + \frac{1}{r}\frac{\partial W_l}{\partial r}\right) + D_{\mathrm{z\ eff}}\left(\frac{\partial^2 W_l}{\partial z^2}\right)\right] \quad (1)$$

This differential equation (eq 1) is solved by assuming (i) the initial moisture content is uniform throughout the solid, (ii) the surface of the solid is at equilibrium with the air for the time considered, and (iii) the shape of the solid remains constant during the drying period considered.

The boundary conditions considered in this study were those related to both the thermodynamic equilibrium and the symmetry of the solid. The initial condition was the sample moisture content at the beginning of drying (Karathanos et al., 1990). In both proposed models, it was assumed that heat transfer proceeds very quickly.

First Model: Separation of Variables Method. Equation 1 can be solved analytically for a constant effective diffusion coefficient, assuming that sample size and shape remain constant (Jayas et al., 1991). The series solution (Perry et al., 1992) corresponded to the product solution for an infinite slab and an infinite cylinder, in which average dimensionless moistures are considered

$$\Psi(t) = \frac{W - W_e}{W_c - W_e} = (\Psi_r)(\Psi_z) \quad (2)$$

where

$$\Psi_r = 4\sum_{i=1}^{\infty}\frac{1}{(b_i)^2}\exp\left[(-b_i)^2\frac{D_{\mathrm{r\ eff}}}{R^2}t\right] \quad (3)$$

$$\Psi_z = 2\sum_{i=1}^{\infty}\frac{1}{(i - 1/2)^2\pi^2}\exp\left[-(i - 1/2)^2\pi^2\frac{D_{\mathrm{z\ eff}}}{Z^2}t\right] \quad (4)$$

By means of the Marquardt least-squares nonlinear regression (Valkó and Vajda, 1989) the effective diffusivity values for the two mass transfer directions for each drying air temperature could be estimated. These estimated diffusivities were fitted to the Arrhenius equation, and D_0 and E_a parameters were calculated.

$$D_{\mathrm{eff}} = D_0 \exp\left(\frac{-E_a}{\mathbf{R}(T + 273)}\right) \quad (5)$$

Second Model: Finite Difference Method. In the second model, a significant change in volume was assumed. Under these circumstances, an unsteady state mass transfer with moving boundary conditions problem should be considered, this being a difficult problem to solve. The effective diffusion coefficients (radial and axial), the average moisture content, and the moisture content profiles were estimated by using a finite difference method (Kotake and Hijikata, 1993).

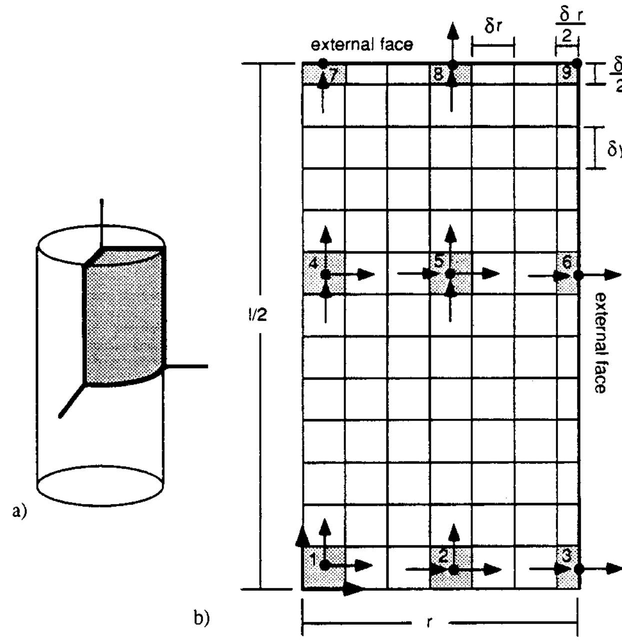

Figure 1. Mass transfer: (a) control volume; (b) longitudinal section of the control volume. Control subvolumes are grouped by transfer characteristics. (●) Nodal points; → mass transfer directions.

For the computational purpose, due to the sample symmetry, the original cylinder could be divided into eight equal parts, delimited by three symmetry planes, one normal to the symmetry axis and the other two chosen among the infinite ones containing that axis and orthogonal among them. The whole piece and the volume considered present the same transfer characteristics. The ratio of the volume/transfer area is also maintained. Therefore, one of these volumes was considered as the control volume (Figure 1).

Model discretization by the finite difference method (Crank, 1975) implies that the original control volume is divided into a constant number of elements. These subvolumes of different size arise from segmenting the height and the radius of the control volume on a given number of intervals. The subvolumes' size reduces due to water losses adjusting their dimension to the moving boundary. Meanwhile, their dry matter remains at a constant value during the process. These subvolumes constitute the so-called *network*. One representative point is chosen in each subvolume (nodal point) where the mass balance will be performed through the finite differences scheme. Nodal points are classified according to their location as inner or boundary nodal points. Nodal points are placed at the center of the subvolume in the case of inner elements and at the surface for the outer elements. Figure 1 shows the volume discretization and the location of the typical inner and boundary nodal points.

Mass losses from the control volume occur only through the two external faces, since symmetry does not allow mass transfer between control volumes. Table 1 shows the different kinds of control subvolumes classified according to their mass transfer characteristics and kind of faces. For classifying purposes in that table the external faces with mass transfer were those in contact with the drying air and the internal faces without mass transfer were those arising from symmetry planes or

Table 1. Mass Transfer Characteristics of Control Subvolumes

control subvolume group	no. of faces: internal, with mass transfer: axial	radial	internal, without mass transfer, axial: symmetry	equilibrium	internal, without mass transfer, radial: symmetry	equilibrium	external, with mass transfer: axial	radial
1	1	1	1	0	0	0	0	0
2	1	2	1	0	0	0	0	0
3	0	1	1	1	0	0	0	1
4	2	1	0	0	0	0	0	0
5	2	2	0	0	0	0	0	0
6	0	1	0	2	0	0	0	1
7	1	0	0	0	0	1	1	0
8	1	0	0	0	0	2	1	0
9	0	0	0	1	0	1	1	1

equilibrium. The rest are the internal faces with mass transfer. It should be noted that due to cylindrical symmetry, only four faces need to be described, two in the axial direction and two in the radial direction (no mass transfer between control volumes). A mass balance applied on a subvolume, in a time interval δt, allows the determination of the local moisture content variation.

An optimization technique, based on the Gauss–Newton method (Valkó et al., 1989), was used for the estimation of the diffusivity values (axial and radial) at different air drying temperatures. The effective diffusivity values were fitted to the Arrhenius equation, and D_0 and E_a parameters were calculated as in the model without shrinkage (eq 5). For parametric estimation, a mixed criterion was used: the sum of relative and absolute square moisture differences in a ratio 1/0.2 (Simal et al., 1994).

MATERIALS AND METHODS

Raw Material and Apparatus. Green bean from the island of Mallorca (*P. vulgaris*) was the raw material used in all experiments. Before drying, green beans of ca. 0.0075 ± 0.0011 m diameter were cut into cylinders and blanched for 15 s by immersion in 100 °C NaOH (1.5 kg/m^3) solution.

Drying experiments were performed in a laboratory scale hot air drier, operating at air mass flux of 3 kg/m^{2}s and temperatures between 30 and 90 °C. The drier used for sample dehydration, described in a previous work (Simal et al., 1996a), was equipped with an automatic temperature controller (±0.1 °C). The air flowed perpendicular to the bed. A monolayer loading was used. The air flow rate was high enough to ensure that mass transfer was controlled by the internal resistance.

Drying Experiments. (a) Experiments were performed with 0.020 m long cylinders at different drying air temperature (30, 50, 70, and 90 °C) to obtain the radial diffusivity. The end surfaces were prevented from air contact with the aid of a silicone film, thus avoiding mass transfer in the axial direction (Mounji et al., 1991).

(b) Experiments were performed with 0.020 m long cylinders at different air drying temperatures (30, 50, 70, and 90 °C) to obtain the axial diffusivity. In this case, mass transfer took place in both directions, axial and radial.

(c) Experiments were performed, on one hand, with 0.020 m long samples at 40, 60, and 80 °C and, on the other hand, with 0.035 m long samples at 60 and 65 °C.

The average room air characteristics were 21 ± 1 °C and 69 ± 5% humidity. Water losses were measured by weighing the basket and its content automatically. The moisture content of the dried product was obtained according to AOAC Method 934.06 (1990). Volume changes were calculated by sudden immersion in distilled water of dried samples with different moisture contents, and measurements of water displacement were collected.

Table 2. D_0 and E_a Values Obtained for the Arrhenius Type Relationship (Equation 5)

model	radial transfer: D_0 (10^4) ($m^2\ s^{-1}$)	E_a (kJ/mol)	r^2	axial transfer: D_0 (10^6) ($m^2\ s^{-1}$)	E_a (kJ/mol)	r^2
without shrinkage	9.04	43.0	0.992	3.62	22.0	0.990
with shrinkage	9.89	43.5	0.988	9.55	24.8	0.999

RESULTS AND DISCUSSION

Shrinkage of the sample during drying was found to be linearly proportional to the change in moisture content (Vagenas et al., 1990). The relationship between volume and moisture content for green beans was obtained:

$$V/V_0 = 0.1331 + 0.0912W \qquad r^2 = 0.988 \tag{6}$$

From the experimental results by measuring the geometric characteristics of the particles during the drying process, it was found that the length and the radius of the cylinder vary for green beans. From these results, the following relationship was obtained for the axial shrinkage:

$$L/L_0 = 0.5744 + 0.0455W \qquad r^2 = 0.984 \tag{7}$$

Shrinkage in the radial direction was determined using eqs 6 and 7.

A constant rate drying period was not detected in the drying kinetics carried out at different drying air temperatures. Drying kinetics in the range of moisture contents considered in this work, from ca. 9.1 to 2 kg of H_2O/kg of dm, showed the existence of only one diffusional period. This type of drying curve has also been reported by different authors (Suarez and Viollaz, 1991; Simal et al., 1994). No case-hardening was observed from the experimental drying curves at the drying conditions employed.

Equilibrium moisture content values (W_e) were obtained with the room air conditions and the moisture isotherms proposed by Samaniego-Esguerra et al. (1991) for green bean. The critical moisture content value (W_c) was the initial moisture content due to the fact that no constant rate period was observed.

Diffusivity Models. By using both proposed models, the figures for the effective diffusion coefficients were identified. The radial diffusivity value ($D_{r\,eff}$) at different temperatures was identified with experiments from set a. By considering these values for $D_{r\,eff}$, axial

Table 3. Diffusivity and Activation Energy Values Proposed by Different Authors

source	foodstuff	T (°C)	D_{eff} (m²/s)	E_a (kJ/mol)
Misra and Young (1980)	soybean	55	3.9×10^{-10}	
Andrieu and Stamatopoulos (1984)	cylindrical pasta	50	3.5×10^{-11}	22.5
Vanegas et al. (1990)	grapes			63.8
Simal et al. (1996b)	grapes	60	6.0×10^{-10}	33.0
Simal et al. (1996a)	green peas	60	1.5×10^{-9}	24.7
this work, model without shrinkage, radial direction	green bean	60	1.6×10^{-10}	43.0
this work, model with shrinkage, radial direction	green bean	60	1.5×10^{-10}	43.5
this work, model without shrinkage, radial direction	green bean	60	1.3×10^{-9}	22.0
this work, model with shrinkage, axial direction	green bean	60	1.2×10^{-9}	24.8

Table 4. Percentage of Explained Variance

T (°C)	L (cm)	model I	model II
Experiments Used in the Parametric Identification			
30	2.0	98.9	99.1
50	2.0	97.1	99.5
70	2.0	96.0	99.2
90	2.0	94.3	99.1
	%var av	96.6 ± 1.7	99.2 ± 0.2
Experiments Not Used in the Parametric Identification			
40	2.0	98.6	99.8
60	2.0	95.2	99.2
80	2.0	94.7	98.8
60	3.5	95.6	98.5
65	3.5	96.0	98.3
	%var av	96.0 ± 1.4	98.9 ± 0.5

diffusivities ($D_{z\ eff}$) were estimated from experiments included in set b.

The temperature dependence was established by fitting D_{eff} values to eq 5. The D_0 and E_a parameters are given in Table 2. Using these parameters, $D_{r\ eff}$ and $D_{z\ eff}$ can be estimated at different temperatures. $D_{z\ eff}$ values estimated through the two proposed models were always higher than $D_{r\ eff}$ values, which represented ca. 15% of $D_{z\ eff}$ values (average value between 30 and 90 °C). Thus, these results confirmed the hypothesis that mass transfer during green bean drying is nonisotropic. The explanation for this observation could lie in the fact that mass transfer resistance in the radial direction can be understood as the result of two different resistances serially connected, one due to the internal tissue and the other one due to the external skin (Sarker et al., 1994). Therefore, $D_{z\ eff}$ figures were lower because there is no skin in the axial direction.

Although no diffusivity and activation energy for green bean were found in the literature, the computed values were in agreement for different foodstuffs (Table 3).

The activation energy figures obtained for the two proposed models were similar for each mass transfer direction. In this way, ln($D_{r\ eff}$) vs the inverse of the absolute temperature plots were straight lines, one for each model, which were practically parallel. The same behavior was observed in the representation of ln($D_{z\ eff}$) vs the inverse of the absolute temperature. Similar results were obtained by Mulet et al. (1989) in carrot drying.

Model Evaluation. The accuracy of the proposed models for the drying falling rate period was evaluated for green beans through the comparison of experimental and simulated drying curves.

In Table 4 are shown the percentages of explained variance (%var) (eq 8) obtained by comparing the average experimental moisture content and those given by the proposed models. The calculation was performed by using the standard deviation of the sample (S_y) and

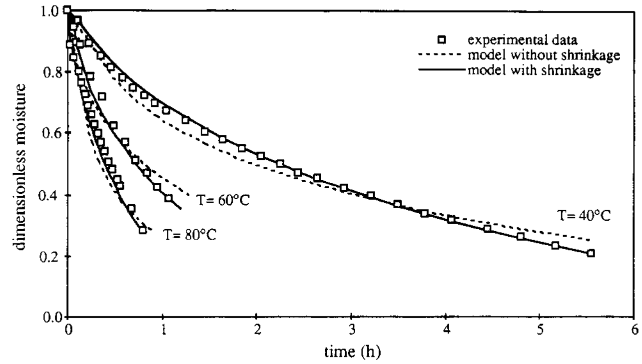

Figure 2. Computed and experimental dimensionless moisture content vs drying time. Experiments were carried out at 40, 60, and 80 °C with 0.020 m long cylinders.

the corresponding estimation (S_{yx}).

$$\%\text{var} = \left[1 - \left(\frac{S_{yx}^2}{S_y^2}\right)\right]^{1/2} \times 100 \qquad (8)$$

The average percentage of the explained variance for the drying curves at different air drying temperatures (30, 50, 70, and 90 °C) using the models without and with shrinkage were 96.6 ± 1.7% and 99.2 ± 0.2%, respectively.

The model with shrinkage provided a good agreement with the experimental drying curves for all air drying temperatures checked and were better than those obtained by the model without shrinkage. According to these results, it was concluded that shrinkage experienced by the samples during drying time could not be neglected to obtain a good representation of drying curves in products like green beans. Similar results were obtained by different authors, who concluded that shrinkage must be taken into account when modeling [Vanegas et al., 1990 (in grapes); Suarez and Viollaz, 1991 (in potato slabs); among others].

The proposed models were further tested by evaluating drying kinetics at different temperatures and particle sizes not used in the parameter estimation experiments. These experiments were those included in set c, performed at 40, 60, and 80 °C with 0.020 m long samples and also at 60 and 65 °C with 0.035 m long samples.

Calculated (using the proposed models) and experimental dimensionless moisture contents are represented in Figures 2 (at 40, 60, and 80 °C with 0.020 m long samples) and 3 (60 and 65 °C with 0.035 m long samples) vs drying time. In these figures, it can be observed that the simplest model provided the worst agreement, especially when the sample length was changed from 0.020 to 0.035 m (%var = 95.8 ± 0.3). Furthermore, the model with shrinkage showed a better agreement of these drying curves (%var = 99.1 ± 0.1).

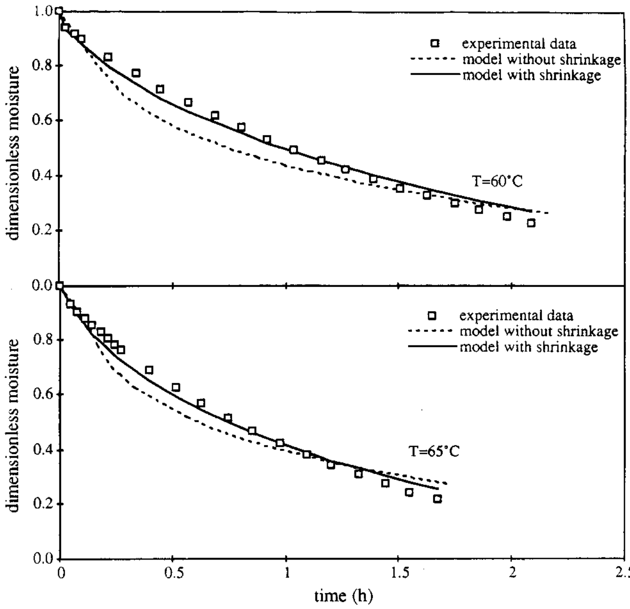

Figure 3. Computed and experimental dimensionless moisture content vs drying time. Experiments were carried out at 60 and 65 °C with 0.035 m long cylinders.

From the average percentages of explained variance obtained by comparing experimental and computed data for the two proposed models (Table 4) it can be concluded that the accuracy using the shrinkage model was considerably higher than that provided by the fixed boundaries model for all of the conditions considered in the experiments. As a consequence, the hypothesis of neglecting sample shrinkage does not allow an adequate simulation of experimental curves.

These two models provide important information about nonisotropic samples behavior with regard to mass transfer phenomena and could be used for different biological and cylindrical products. Moreover, the model with shrinkage is adequate to describe the effective diffusion coefficient variation and water losses even when sample shrinkage during the process is significant.

ABBREVIATIONS USED

D_{eff}, effective diffusivity, m^2/s; D_0, preexponential factor Arrhenius equation, m^2/s; $D_{r\,eff}$, radial effective diffusivity, m^2/s; $D_{z\,eff}$, axial effective diffusivity, m^2/s; E_a, activation energy, kJ/mol; L, half-length of the solid, m; L_0, initial half-length of the solid, m; r, r axis distance, m; R, radius of the cylinder; R, m; **R**, gas constant, 8.3 J/mol K; S_y, standard deviation (sample), (g of water/g of dm)^2; S_{yx},standard deviation (estimation), (g of water/g of dm)^2; t, time, s; T, air temperature, °C; V, volume of the solid, m^3; V_0, initial volume of the solid, m^3; W, average moisture content, kg of water/kg of dm; W_c, critical moisture content, kg of water/kg of dm; W_e, equilibrium moisture content, kg of water/kg of dm; W_l, local mositure content, kg of water/kg of dm; z, z axis distance, m; Z, half-length of the cylinder, m; β_v, successive solutions of $Jo(\beta v) = 0$; Ψ, dimensionless moisture; Ψ_r, radial dimensionless moisture; Ψ_z, axial dimensionless moisture; %var, percentage of explained variance.

LITERATURE CITED

Aguilera, J. M.; Stanley, D. W. *Microstructural Principles of Food Processing and Engineering*; Elsevier Applied Sciencie Publishers: New York, 1990.

Andrieu, J.; Stamatopoulos, A. Diffusion model applied to pasta drying kinetics. Presented at the International Drying Symposium '84, Boston, MA, 1984.

AOAC *Official Methods of Analysis of the Association of Official Analytical Chemists*; Arlington, VA, 1990; No. 934.06.

Crank, J. *The Mathematics of the Diffusion*; Oxford University Press: London, 1975.

Fusco, A. J.; Avanza, J. R.; Aguerre, R. J.; Gabitto, J. F. A diffusional model for drying with volume change. *Drying Technol.* **1991**, *9* (2), 397–417.

Holland, B.; Welch, A. A.; Unwin, I. D.; Buss, D. H.; Paul, A. A.; Southgate, D. A. T. *The Composition of Foods*; McCance and Widdowson's; The Royal Society of Chemistry: London, U.K., 1991.

Jayaraman, K. S.; Das Gupta, D. K. Dehydration of fruits and vegetables. Recent developments in priciples and techniques. *Drying Technol.* **1992**, *10* (1), 1–50.

Jayas, D. S.; Cenkowski, S.; Pubis, S.; Muir, W. E. Review of thin-layer drying and wetting equations. *Drying Technol.* **1991**, *9* (3), 551–588.

Jomaa, W; Aregba, W.; Puiggali, J. R. Drying of highly shrinking products: application to gels. In *Drying '91*; Mujumdar, A. S., Filkova, I., Eds.; Elsevier: New York, 1991.

Karathanos, V. T.; Villalobos, G.; Saravacos, G. D. Comparison of two methods of estimation of the effective moisture diffusivity from drying data. *J. Food Sci.* **1990**, *55* (1), 218–231.

Ketelaars, A. A. J.; Pel, L.; Coumans, W. J.; Kerkhof, P. J. A. M. Drying kinetics. A comparison of diffusion coefficients from moisture concentration profiles and drying curves. *Chem. Eng. Sci.* **1995**, *50* (7), 1887–1191.

Kiranoudis, C. T.; Maroulis, Z. B.; Marinos-Kouris, D. Model selection in air drying of foods. In *Drying '92*; Mujumdar, A. S., Ed.; Elsevier: New York, 1992.

Koponen, H. Moisture diffusion coefficients of wood. In *Drying '87*; Mujumdar, A. S., Ed.; McGill University: Montreal, Canada, 1987.

Kotake, S.; Hijikata, K. *Numerical Simulations of Heat Transfer and Fluid Flow on a Personal Computer*; Elsevier: Amsterdam, 1993.

Misra, R. N.; Young, J. H. Numerical solution of simultaneous moisture diffusion and shrinkage during soybean drying. *Trans. ASAE* **1980**, 1277–1282.

Mounji, H.; El Kouali, M.; Bouzon, J.; Vergnaud, J. M. Modelling of the drying process of wood in 3-dimensions. *Drying Technol.* **1991**, *9* (5), 1295–1314.

Mulet, A.; Berna, A.; Rosselló, C. Drying of carrots. I. Drying models. *Drying Technol.* **1989**, *7*, 537–557.

Perry, H. R.; Green, D.; Maloney, J. O. *Perry*'s *Chemical Engineering Handbook*, 6th ed.; McGraw-Hill: New York, 1992.

Rosselló, C.; Cañellas, J.; Simal, S.; Berna, A. Simple mathematical model to predict the drying rates of potato. *J. Agric. Food Chem.* **1992**, *40*, 2374–2378.

Samaniego-Esguerra, C. M.; Boag, I. F.; Robertson, G. L. Comparison of regression methods for fitting the GAB model to the moisture isotherms of some dried fruit and vegetables. *J. Food Eng.* **1991**, *13*, 115–133.

Sarker, N. N.; Kunze, O. R.; Strouboulis, T. Finite element simulation of rough rice drying. *Drying Technol.* **1994**, *12*(4), 761–775.

Schrader, G. W.; Litchfield, J. B. Moisture profiles in a model food gel during drying: measurement using magnetic resonance imaging and evaluation of the Fickian model. *Drying Technol.* **1992**, *10* (2), 295–332.

Simal, S.; Rosselló, C.; Berna, A.; Mulet, A. Heat and mass transfer model for potato drying. *Chem Eng. Sci.* **1994**, *49* (22), 3739–3744.

Simal, S.; Mulet, A.; Tarrazó, J.; Rosselló, C. Drying models for green peas. *Food Chem.* **1996a**, *55* (2), 121–128.

Simal, S.; Mulet, A.; Catalá, P. J.; Cañellas, J.; Rosselló, C. Moving boundary model for simulation moisture movement in grapes. *J. Food Sci.* **1996b**, *61* (1), 157−160.

Suarez, C.; Viollaz, P. E. Shrinkage effect on drying behavior of potato slabs. *J. Food Eng.* **1991**, *13*, 103−114.

Vagenas, G. K.; Marinos-Kouris, D.; Saravacos, G. D. An analysis of mass transfer in air drying foods. *Drying Technol.* **1990**, *8* (2), 323−342.

Vagenas, G. K.; Marinos-Kouris, D. Drying kinetics of apricots. *Drying Technol.* **1991**, *9* (3), 735−752.

Valkó, P.; Vajda, S. *Advanced Scientific Computing in BASIC with Applications in Chemistry, Biology and Pharmacology*; Elsevier: Amsterdam, 1989.

Welty, J. R.; Wicks, C. E.; Wilson, R. E. *Fundamentals of Momentum, Heat and Mass Transfer*; Limusa: Mexico, 1993, Chapter 25, pp 571−585.

Yoshida, M.; Imakoma, H.; Okazaki, M. Characteristic functions for the drying of non-hygroscopic porous slab with a constant body temperature. *J. Chem. Eng. Jpn.* **1990**, *23* (1), 58−63.

Received for review July 18, 1996. Revised manuscript received November 7, 1996. Accepted November 8, 1996.[⊗] We acknowledge the financial support of CICYT (ALI94-0565-C03).

JF960534C

[⊗] Abstract published in *Advance ACS Abstracts,* January 1, 1997.